Nanoparticles of Conjugated Polymers Prepared from Phase-Separated Films of Phospholipids and Polymers for Biomedical Applications

ARTICLE *in* ADVANCED MATERIALS · JULY 2014

Impact Factor: 17.49 · DOI: 10.1002/adma.201400906 · Source: PubMed

13 AUTHORS, INCLUDING:

Tae Joo Shin
Ulsan National Institute of Science and Tec…
127 PUBLICATIONS **2,530** CITATIONS
SEE PROFILE

Joonhyuck Park
Pohang University of Science and Technology
15 PUBLICATIONS **311** CITATIONS
SEE PROFILE

Tae Jung Park
Chung-Ang University
126 PUBLICATIONS **1,536** CITATIONS
SEE PROFILE

Pil J. Yoo
Sungkyunkwan University (SKKU)
85 PUBLICATIONS **2,989** CITATIONS
SEE PROFILE

Nanoparticles of Conjugated Polymers Prepared from Phase-Separated Films of Phospholipids and Polymers for Biomedical Applications

*Jungju Yoon, Jungheon Kwag, Tae Joo Shin, Joonhyuck Park, Yong Man Lee, Yebin Lee, Jonghyup Park, Jung Heo, Chulmin Joo, Tae Jung Park, Pil J. Yoo, Sungjee Kim, and Juhyun Park**

Nanoparticles and nanodots (d <~30 nm) of conjugated polymers have received considerable attention over the last decade in an effort to realize brighter luminescence, facile processing, and enhanced device efficiency.[1] For example, conjugated polymer nanospheres have enhanced the device performance of organic photovoltaic devices by forming nanoscale domains in thin films.[2] In biology and medicine, densely packed nanospheres of conjugated polymers have exhibited higher fluorescence lifetime, emission rates, and photostability than single molecular dyes.[3] Thus, with surface functionalization, bioconjugation, or hybridization, nanospheres have been explored for biological applications such as labeling,[4] imaging,[5] sensing,[6] and drug delivery.[7]

Technologies to prepare nanospheres of conjugated polymers can be categorized into two major methods: dispersion of already prepared polymers and polymerization from monomers in dispersion media, as recently reviewed in the literature.[1] The dispersion techniques include the emulsification of polymer solutions in excess water with surfactants, followed by extraction of the organic solvents, which are immiscible with water and volatile,[8] and the nanoprecipitation of polymers dissolved in organic solvents to water where the organic solvents and water are miscible.[3,9] These processing techniques make it possible to use almost all of the commercially available conjugated polymers that are soluble in organic solvents, thereby avoiding laborious synthesis/modification steps in order to introduce ionic functionalities for preparing conjugated polyelectrolytes. The dispersion polymerization route typically employs monomers, polymeric steric stabilizers, and solvents in which the monomers are miscible but the resulting polymers are insoluble. This methodology enables the preparation of nanoparticles of conjugated polymers that are difficult to dissolve in solvents. A variety of polymers such as polypyrroles,[10] polyanilines,[11] polyacetylenes,[12] polythiophenes,[13] and polyphenylenevinylenes[14] could be prepared to form nanospheres by directly polymerizing monomers in heterophase systems.

Despite the widespread use of conjugated polymer nanoparticles for biological applications, current technologies still need laborious processes to introduce functionalities, typically amines or carboxylic acid, to nanoparticles, which are necessary to conjugate cell specific ligands, inorganic nanomaterials such as quantum dots or polyethylene glycols to prevent non-specific bindings in vivo. For examples, the incorporation of functionalities to the nanoparticles of conjugated polymers requires to synthesize new polymers.[15] Pre-functionalization is still a prerequisite even for the nanoprecipitation technology.[16] There have been limited reports for technologies in which the pre-functionalization of conjugated polymers is not necessary.[17]

In this contribution, we introduce a method of preparing nanoparticles of conjugated polymers from phase-separated thin films, which is conceptually distinct from technologies reported up to the present. We prepared phase-separated thin films of poly[*2,6*-(4,4-bis-(2-ethylhexyl)-4*H*-cyclopenta[2,1-b;3,4-b′]-dithiophene)-*alt*-4,7-(2,1,3-benzothiadiazole]] (PCPDTBT) and a phospholipid, and then broke the thin films to form nanoparticles of conjugated polymers. When PCPDTBT and a phospholipid are dissolved in a cosolvent and the cosolvent is evaporated, it is clearly anticipated that the resulting films will show a phase-separated morphology because of immiscibility between the hydrophobic PCPDTBT and the polar heads of the phospholipids. Furthermore, nanometer-scale associations can be formed when the alkyl tail length of the phospholipid is comparable to the alkyl side chain length of the conjugated polymer. Ultrasonication of the solution after adding water enables the water molecules to penetrate into the thin films due to the existence of polar regions in the phospholipid heads, thus breaking the thin films and ultimately dispersing nanoparticles of conjugated polymers into the aqueous media. In this study,

J. Yoon, Y. Lee, J. Park, Prof. T. J. Park, Prof. J. Park
School of Chemical Engineering and Materials Science
Department of Chemistry
Chung-Ang University
Seoul 156–756, Republic of Korea
J. Kwag, J. Park, Dr. T. J. Shin, Prof. S. Kim
Department of Chemistry
Pohang Accelerator Laboratory
Pohang University of Science and Technology
Pohang 790–784, Republic of Korea
E-mail: jpark@cau.ac.kr
Y. M. Lee, Prof. P. J. Yoo
School of Chemical Engineering and SKKU
Advanced Institute of Nanotechnology (SAINT)
Sungkyunkwan University
Suwon 440–746, Republic of Korea
J. Heo, Prof. C. Joo
School of Mechanical Engineering
Yonsei University
Seoul 120–749, Republic of Korea

DOI: 10.1002/adma.201400906

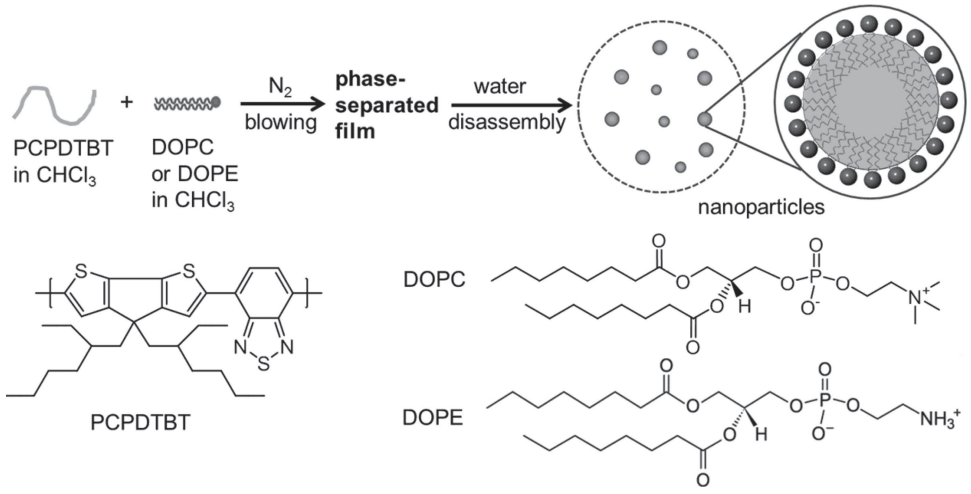

Figure 1. A schematic illustration of formation of water-dispersed conjugated polymer nanoparticles.

we use PCPDTBT, 1,2-dioctanoyl-*sn*-glycero-3-phosphocholine (DOPC) and 1,2-dioctanoyl-*sn*-glycero-3-phosphoethanolamine (DOPE), and demonstrate that the idea delineated above and shown in **Figure 1** can be realized. We first demonstrate that the phase-separation between the conjugated polymer and a phosphocoline-based lipid, and subsequent nanoparticle formation upon disassembly is possible by using PCPDTBT and DOPC, avoiding any excess synthetic step together with high, controllable particle yield via an easy, robust, and reproducible process. We further show that nanoparticles with primary amines at their surface can be formed by employing PCPDTBT and DOPE, thus widely opening applications for biology and medicine by post-functionalization on demands.

Films of PCPDTBT and DOPC were deposited on silicon substrates and the phase-separated morphology was investigated by AFM analysis. **Figure 2**a and 2b show AFM images of the thin films prepared at a polymer-to-lipid molar ratio of 1:5. The tapping-mode image in Figure 2a shows topological features that resemble micrometer-scale aggregates. In the phase-mode image in Figure 2b, it is confirmed that the aggregates have a different phase from the surrounding region with irregular patterns. The portion of these aggregated domains decreased with increasing polymer-to-lipid molar ratio (1:1, 1:2, 1:10, and 1:30, Figure S1). These results clearly indicate that aggregated domains are assemblies of PCPDTBT and DOPC and that the surrounding region comprises excess lipid molecules, proving the formation of phase-separated thin films due to immiscibility between the polar heads of DOPC and the hydrophobic conjugated polymer.

After adding deionized water to the phase-separated films, the shattering of the films by penetration of water molecules into the polar region of the thin films with ultrasonication was observed by SEM imaging with differing ultrasonication times. Figure 2c shows that the micrometer-scale aggregates become an association of nanoparticles after 3 h ultrasonication, indicating that the microaggregates are nanoassemblies of PCPDTBT and DOPC. SEM image and particle analysis data in Figures 2d and 2e, respectively, were obtained from PCPDTBT nanoparticles after 4 h ultrasonication, showing the films finally broken into nanoparticles. Particle size analysis after centrifuging and redispersing the nanoparticles in water shows an average diameter of 58.8 ± 21.2 nm. In all the polymer-to-lipid molar ratios used in our study, nanoparticles of PCPCTBT were successfully formed from phase-separated thin films. In addition, only when DOPC or DOPE with C8 alkyl tails was

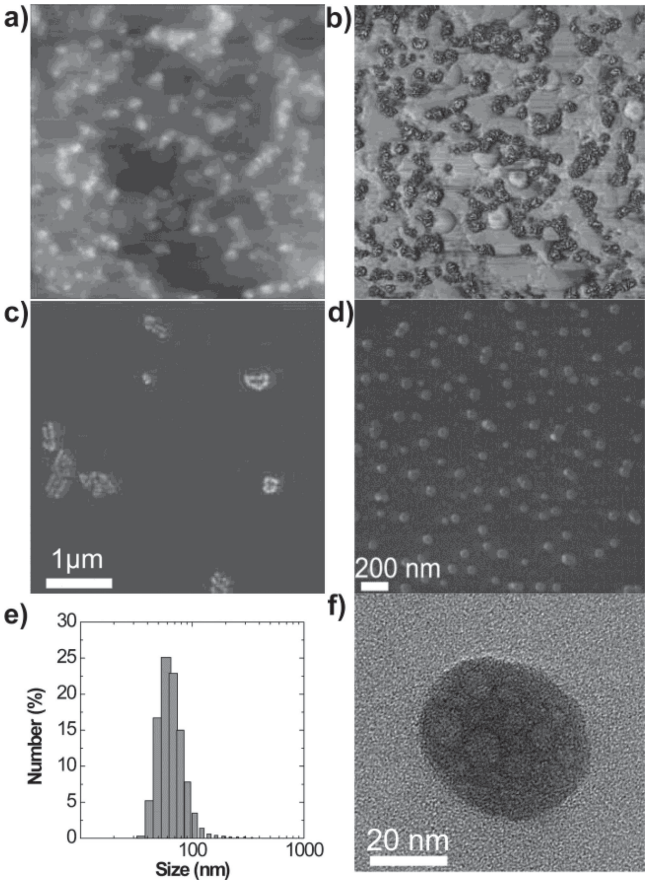

Figure 2. (a) Topological and (b) phase-mode AFM images of dry thin films of PCPDTBT and DOPC with sample area 10 × 10 μm^2, SEM images of disassembled films after (c) 3 h and (d) 4 h ultrasonication in water, (e) particle analysis data, and (f) a TEM image of PCPDTBT nanoparticles.

employed, independent, isolated PCPDTBT nanoparticles were most effectively produced. The uniform formation of PCPDTBT nanoparticles was not successful when we used phosphocholine-based lipids with different carbon numbers of alkyl tails (C4, C5, C6, C7, C9, and C10, Figure S2), proving the existence of nanomorphology due to comparable lengths between polymer side chains and lipid tails.

The assembly structure of PCPDTBT with DOPC in the nanoparticles was characterized by measuring the zeta potential and by TEM images. The zeta potential values measured for the nanoparticle solution was −22 mV. This value is similar to that measured for unilamellar vesicles prepared from phosphocholine-based lipid molecules.[18] This result indicates that the assembly structure based on the charge compensation of the choline cation and the phosphate anion in the polar head of DOPC, which is schematically illustrated in the literature,[19] is seemingly formed on the surface of PCPDTBT nanoparticles. The high-resolution TEM image provides additional interesting results. As shown in Figure 2f, a PCPDTBT nanoparticle exhibits bright dots with diameters of approximately 10 nm. The bright dots in the TEM image, which reflect spherical structures with low electron densities, suggest that smaller DOPC vesicles are embedded in PCPDTBT nanoparticles. These interesting nanostructures were not universally formed for all prepared nanoparticles, as observed by TEM imaging (Figure S3). However, the existence of these structures confirms a plausible mechanism for the formation of nanoparticles. Microaggregates are nanosassemblies of PCPDTBT and DOPC, and water molecules can penetrate into the aggregates through the polar region during ultrasonication after adding water. The end result is the disassembly of the films, generating water-dispersed nanoparticles of PCPDTBT that are covered with lipid polar heads and sometimes bear smaller lipid nanovesicles.

The closely packed molecular structures in the PCPDTBT nanoparticles were confirmed by the solution WAXS profile shown in **Figure 3**a, and the UV absorption and photoluminescence spectra illustrated in Figure 3b and 3c. It is known that PCPDTBT is amorphous in the solid state of thin films.[20] However, our PCPDTBT nanoparticles have a strong short-range association, as proven in the WAXS profile shown in Figure 3a, in which the d-spacing at 3.14 Å and 2.24 Å is clearly shown, although the profile does not present well developed diffraction peaks related to crystalline structures. The d-spacing at 3.14 Å is well coincident with the displacement distance of conjugated backbones and that at 2.24 Å is assigned for the stacking of alkyl chains.[21] The reason for this assignment is because (011) and (310) planes with a d-spacing of 2.26 and 2.21 Å appears for the stacking of alkyl chains in crystalline polyethylenes.[21] This closely associated molecular structure produces a characteristic absorption peak at 780 nm, as shown in Figure 3b. This kind of red-shifted absorption peak was also discovered in thin films of active layers for polymeric photovoltaic cells due to close association among conjugated backbones influenced by alkyl side chains.[20,22] The enhancement of the absorption peak at a longer wavelength suggests an increase in π-π interactions with the closely associated molecular structures in the PCPDTBT nanoparticles. In comparison, the maximum absorption occurred at 718 nm (the dashed line in Figure 3b) when PCPDTBT was dissolved in chloroform at a concentration of 0.1 mg/mL, indicating that there was no significant association between the polymer molecules. Correspondingly, photoluminescence from PCPDTBT nanoparticles excited at 780 nm peaked at 890 nm in the near-infrared region, whereas that from the chloroform solution of PCPDTBT excited at 718 nm showed a maximum intensity at 780 nm, as shown in Figure 3c.

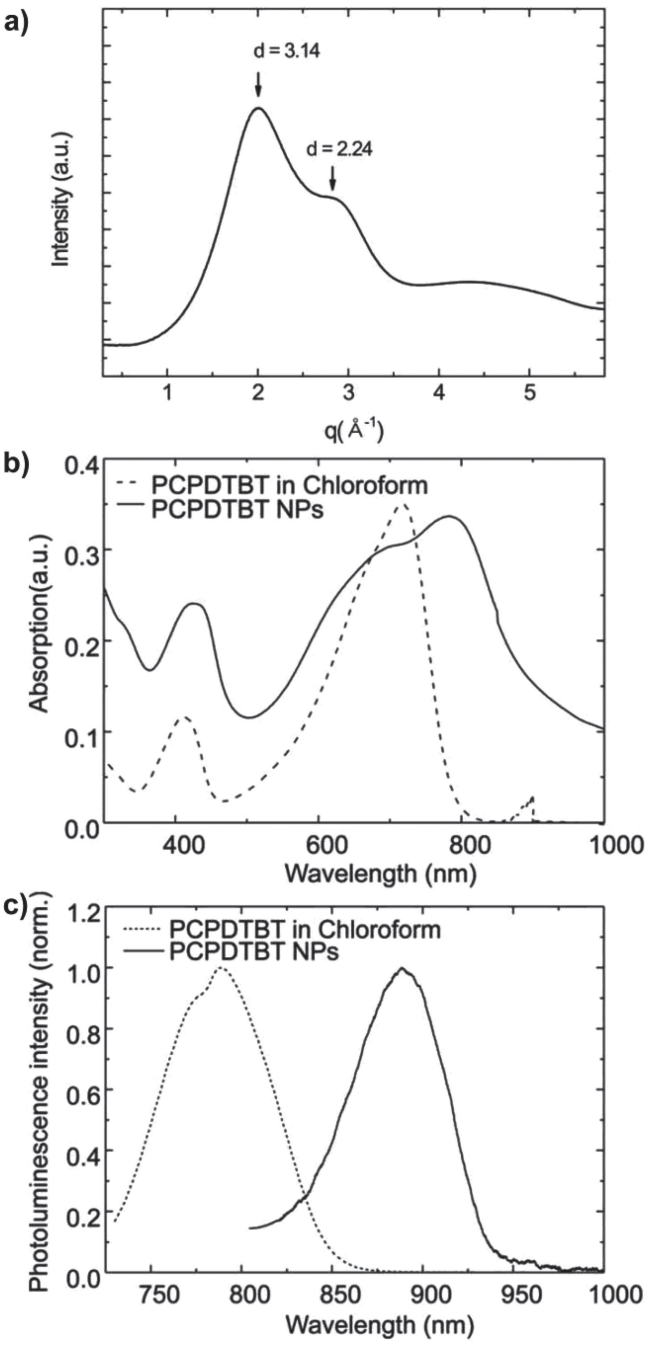

Figure 3. (a) Wide-angle X-ray scattering profile of PCPDTBT nanoparticle solution, (b) UV-visible, and (c) photoluminescence spectra of PCPDTBT nanoparticles dispersed in water (solid line) and PCPDTBT dissolved in chloroform (dashed line for absorption spectrum and dotted line for photoluminescence spectrum).

To examine the applicability of PCPDTBT nanoparticles for biology, we observed the cellular uptake by confocal microscopy (**Figure 4**a and S4a), cytotoxicity effect (Figure S4b), and photothermal therapeutic effects (Figure 4b and 4c). It appears that cell viability at 0.1 and 0.05 mg/mL PCPDTBT nanoparticle concentrations is comparable to that of the controlled test without nanoparticles. The cytotoxicity effect was the best for nanoparticles prepared at 1:5 of polymer to lipid ratio. The possibility of using PCPDTBT nanoparticles as a photothermal therapeutic agent was first examined by measuring the optical phase changes of a 1310 nm light reflecting from a quartz cuvette filled with aqueous nanoparticle solutions at the concentrations of 0.4, 0.7, and 1.0 mg/ml (see Figure S5 for experimental setup.[23]). We measured the phase of the interference between the reflections from the top and bottom surfaces of the inner chamber. Upon irradiating the solutions with an 808 nm laser, the variation of local densities (or refractive index of the solution) was induced, and thus the optical phase differences between the reflections from the top and bottom surfaces varied with increasing nanoparticle concentrations (Figure 4b). These results indicate that heat is generated from the nanoparticles surrounded by water due to radiationless decay and its influence on local densities. In vitro experiments using HeLa cell medium and PCPDTBT nanoparticles clearly showed the photothermal therapeutic effect. As shown in Figure 4c, blue-stained dead cells appeared from a laser power of 8 W/cm^2 at a nanoparticle concentration of 0.1 mg/mL, proving the photothermal therapeutic effect of PCPDTBT nanoparticles.

PCPDTBT nanoparticles show good performance both as a fluorescence imaging agent and as a photothermal therapeutic agent because of their moderate quantum yield. The measured quantum yields of single chain PCPDTBT dissolved in non-polar solvents of toluene and chloroform (λ_{ex} = 758 nm) were 0.50 and 0.41, respectively, in respect to IR-780. Interestingly, the quantum yield of PCPDTBT nanoparticles dispersed in deionized water was 0.39 (λ_{ex} = 789 nm), a minimal decrease considering radiationless decay to the polar medium of water. This quantum yield value of the nanoparticles, which is comparable to that of single-chain PCPDTBT in non-polar solvents, suggests the minimal presence or absence of water molecules inside the nanoparticles and multifunctional applications for imaging and therapy. It should be mentioned that the photothermal activity of our PCPDTBT nanoparticles is not the best among currently available nanomaterials as photothermal agents,[24] which include gold nanorods, carbon nanotubes, and organic dyes such as porphyrin. However, the photothermal activity can be further enhanced by attaching a quenching agent if one plans to use the nanoparticles solely as a photothermal agent. Also, our technology provides a new way of preparing photothermal agents based on new developments in conjugated polymers.[25]

The applicability of PCPDTBT nanoparticles for bioconjugation was investigated by the conventional streptavidin–biotin association. The PCPDTPT nanoparticles have primary amine functionalities on their surface when DOPE is employed during the nanoparticle preparation process. Thus, the formation of amide bonds by reacting with biotin–NHS becomes convenient. The resulting PCPDTBT–biotin nanoparticles can be associated on the surface of polystyrene beads (d = 2.8 μm) coated

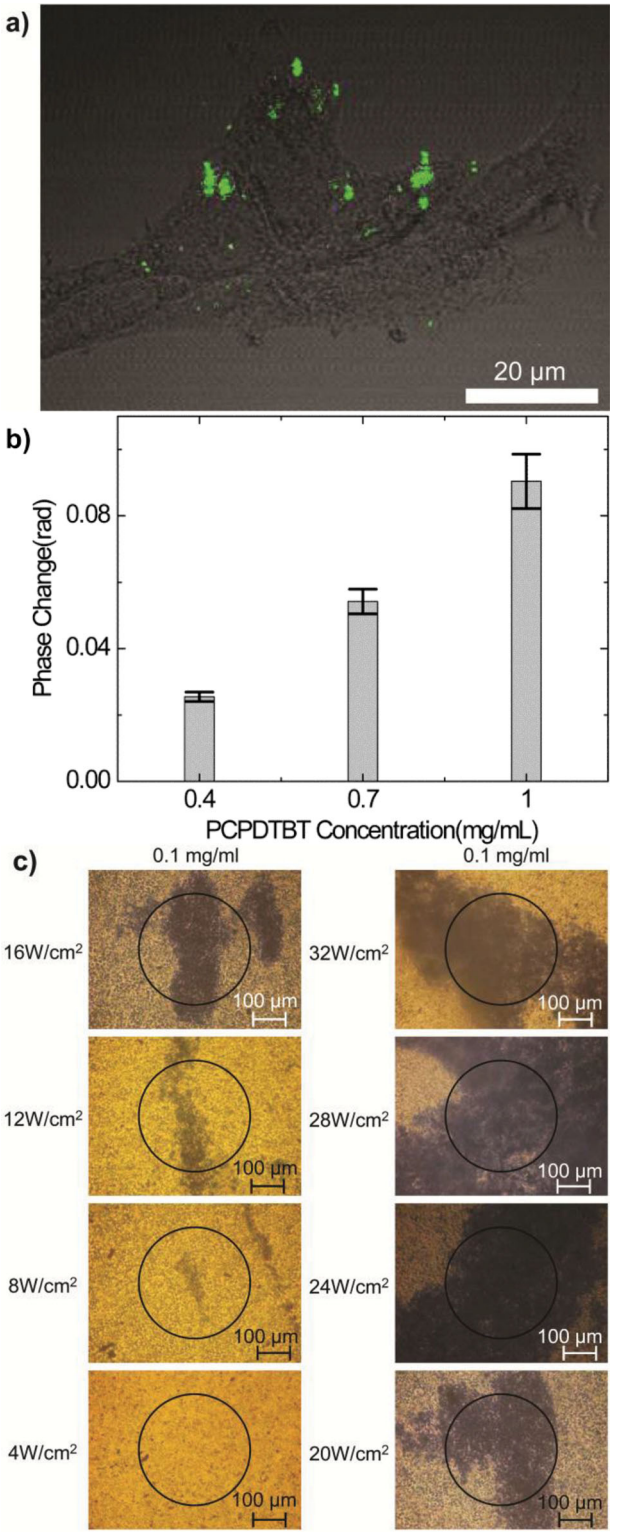

Figure 4. (a) Fluorescence image of HeLa cells after uptaking nanoparticles, (b) Optical phase changes with increasing solid contents of PCPDTBT nanoparticles, and (c) photothermal therapeutic effects observed by staining dead HeLa cells with Trypan blue after irradiating them with a laser at 808 nm for 5 min. The circles show the irradiated areas.

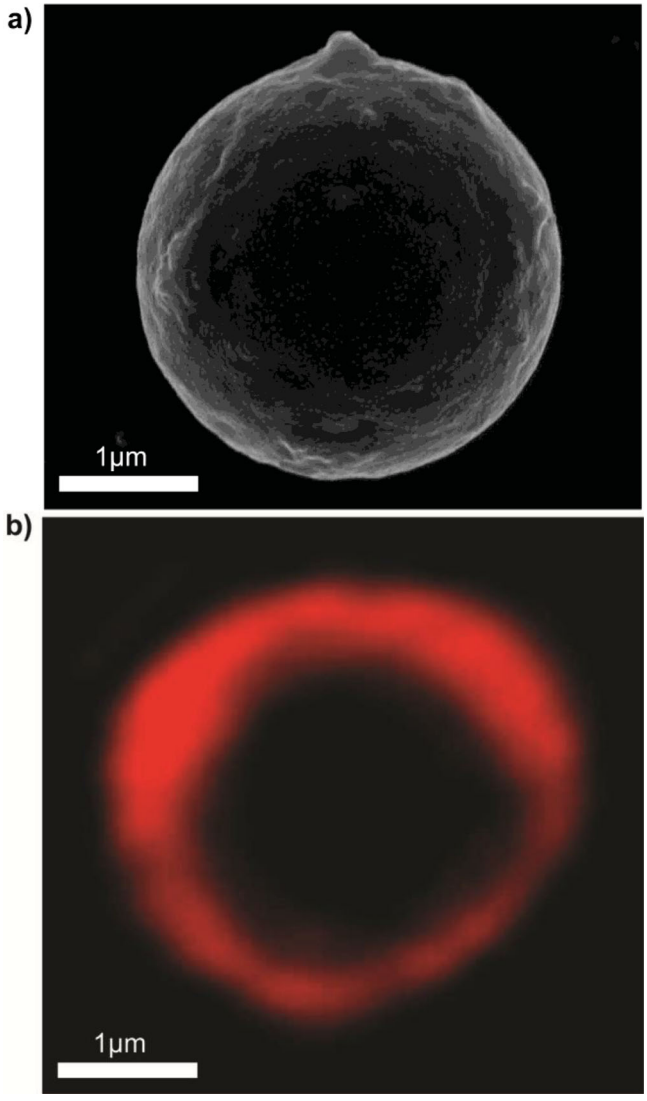

Figure 5. (a) SEM and (b) confocal microscopy images of polystyrenee beads coated with streptavidin after conjugating biotin-attached PCPDTBT nanoparticles.

with streptavidin. The SEM image in **Figure 5**a demonstrates that PCPDTBT–biotin nanoparticles successfully cover the polystyrene–streptavidin beads. The streptavidin–biotin association is also clearly confirmed by the confocal microscopy image, in which photoluminescence is solely from PCPDTBT nanoparticles, thereby giving a ring-type fluorescence image, as shown in Figure 5b.

In summary, nanoparticles of conjugated polymers were prepared from phase-separated nanoassemblies in films of polymers and phospholipids by breaking the films with ultrasonication in water, which is a novel approach for preparing nanoparticles/nanodots of conjugated polymers, and which is clearly distinguished from current technologies. The resulting lipid-assembled nanoparticles of conjugated polymers contain smaller lipid vesicles, and present strong absorption at longer wavelengths. The lipid-assembled nanoparticles of conjugated polymers can thus be used both as fluorescence imaging probes and photothermal therapeutic agents employing near-infrared light. Also, the lipid nanovesicles confined in polymer nanoparticles and the bioconjugation of the nanoparticles using primary amine chemistry suggest the versatility of lipid-assembled nanoparticles of conjugated polymers in that they can be combined with various functionalities such as cell-specific ligands, organic/inorganic nanomaterials and polyethylene glycols for in vivo applications.

Experimental Section

Nanoparticle Preparation: 1 mg of PCPDTBT (MW = 34 kDa, PDI = 2.1, MW on a repeat unit basis = 534.845 g/mol, One Materials, Inc., Quebec, Canada) was dissolved in 10 mL of chloroform. After placing 1 mL of the resulting polymer solution (0.1 mg PCPDTBT/mL, 18.7 μmol on a repeat unit basis) in a separate vial, 56.9 mg of DOPC (93.5 μmol, MW = 509.614 g/mol, Avanti Polar Lipids, Inc., Alabama, USA) was added and dissolved with ultrasonication for 5 min. The molar ratio of the polymer to the lipid was 1:5. Solutions with polymer-to-lipid molar ratios of 1:1, 1:2, 1:10, and 1:30 were also prepared through the same procedure. Then the solvent of the final solution was completely removed with nitrogen blowing in an oil bath at 32 °C to avoid rapid precipitation due to heat loss during evaporation. The samples were further dried in vacuum at room temperature for 12 h. Finally, the thin film that formed on the inner wall of the vial was shattered to nanoparticles by adding 1 mL of deionized water and ultrasonicating the sample for 4 h. The temperature of the sonication bath was controlled to remain below 40 °C to prevent possible damage to the polymers by a temperature increase during ultrasonication. Nanoparticles with surface primary amines were prepared via the same procedure except the use of DOPE instead of DOPC at a polymer to lipid ratio of 1:1. Also, when water was added to the phase-separated films of PCPDTBT and DOPE, water pH was adjusted to 3.5 to ensure the complete ionization of primary amines in DOPE, thereby promoting the disassembly of dry films with ultrasonication. See supporting information for further experimental details about nanoparticle characterization, confocal imaging of cellular uptake, cytotoxicity tests, ablation of HeLa cells by photothermal effect and bioconjugation.

Supporting Information

Supporting Information is available from the Wiley Online Library or from the author.

Acknowledgements

This study was supported by grants of the Korea Research Foundation (Grant No. 2013R1A1A2058816 and 2013056343) and the Korean Health Technology R&D Project, Ministry of Health & Welfare, Republic of Korea (Grant No. HN10C0032020013).

Received: February 26, 2014
Revised: March 26, 2014
Published online: May 2, 2014

[1] a) J. Pecher, S. Mecking, *Chem. Rev.* **2010**, *110*, 6260; b) C. Wu, D. T. Chiu, *Angew. Chem. Int. Ed.* **2013**, *52*, 3086.
[2] T. Kietzke, D. Neher, K. Landfester, R. Montenegro, R. Guntner, U. Scherf, *Nat. Mater.* **2003**, *2*, 408.
[3] a) X. J. Zhao, R. P. Bagwe, W. H. Tan, *Adv. Mater.* **2004**, *16*, 173; b) H. Ow, D. R. Larson, M. Srivastava, B. A. Baird, W. W. Webb,

U. Wiesner, *Nano Lett.* **2005**, *5*, 113; c) L. Wang, K. M. Wang, S. Santra, X. J. Zhao, L. R. Hilliard, J. E. Smith, J. R. Wu, W. H. Tan, *Anal. Chem.* **2006**, *78*, 646.
[4] M. Green, P. Howes, C. Berry, O. Argyros, M. Thanou, *Proc. Math. Phys. Eng. Sci.* **2009**, *465*, 2751.
[5] X. L. Feng, Y. L. Tang, X. R. Duan, L. B. Liu, S. Wang, *J. Mater. Chem.* **2010**, *20*, 1312.
[6] Z. Y. Tian, J. B. Yu, C. F. Wu, C. Szymanski, J. McNeill, *Nanoscale* **2010**, *2*, 1999.
[7] X. L. Feng, F. T. Lv, L. B. Liu, H. W. Tang, C. F. Xing, Q. O. Yang, S. Wang, *ACS Appl. Mater. Interfaces* **2010**, *2*, 2429.
[8] K. Landfester, R. Montenegro, U. Scherf, R. Guntner, U. Aswapirom, S. Patil, D. Neher, T. Kietzke, *Adv. Mater.* **2002**, *14*, 651.
[9] a) C. F. Huebner, R. D. Roeder, S. H. Foulger, *Adv. Funct. Mater.* **2009**, *19*, 3604; b) C. Wu, C. Szymanski, Z. Cain, J. McNeill, *J. Am. Chem. Soc.* **2007**, *129*, 12904.
[10] R. B. Bjorklund, B. Liedberg, *Chem. Commun.* **1986**, 1293.
[11] J. Jang, *Adv. Polym. Sci.* **2006**, *199*, 189.
[12] J. Edwards, R. Fisher, B. Vincent, *Makromol. Chem. Rapid Commun.* **1983**, *4*, 393.
[13] S. J. Lee, J. M. Lee, I. W. Cheong, H. Lee, J. H. Kim, *J. Polym. Sci., Part A: Polym. Chem.* **2008**, *46*, 2097.
[14] J. Pecher, S. Mecking, *Macromolecules* **2007**, *40*, 7733.
[15] Y.-H. Chan, F. Ye, M. E. Gallina, X. Zhang, Y. Jin, I.-C. Wu, D. T. Chiu, *J. Am. Chem. Soc.* **2012**, *134*, 7309.
[16] K. Petkau, A. Kaeser, I. Fischer, L. Brunsveld, A. P. H. J. Schenning, *J. Am. Chem. Soc.* **2011**, *133*, 17063.
[17] P. Howes, A, J. Levitt, K. Suhling, M. Hughes, *J. Am. Chem. Soc.* **2010**, *132*, 3989.
[18] a) K. Makino, T. Yamada, M. Kumara, T. Oka, H. Ohshima, T. Kondo, *Biophys. Chem.* **1991**, *41*, 175; b) F. Pincet, S. Cribier, E. Perez, *Eur. Phys. J. B* **1999**, *11*, 127.
[19] a) L. E. Garner, J. Park, S. M. Dyar, A. Chworos, J. J. Sumner, G. C. Bazan, *J. Am. Chem. Soc.* **2010**, *132*, 10042; b) Y. Lee, I. Yang, J. E. Lee, S. Hwang, J. W. Lee, S.-S. Um, T. L. Nguyen, P. J. Yoo, H. Y. Woo, J. Park, S. K. Kim, *J. Phys. Chem. C* **2013**, *117*, 3298.
[20] J. Peet, J. Y. Kim, N. E. Coates, W. L. Ma, D. Moses, A. J. Heeger, G. C. Bazan, *Nat. Mater.* **2007**, *6*, 497.
[21] a) H.-Y. Chen, J. Hou, A. E. Hayden, H. Yang, K. N. Houk, Y. Yang, *Adv. Mater.* **2010**, *22*, 371; b) K. Tashiro, I. Tanaka, T. Oohara, N. Niimura, S. Fujiwara, T. Kamae, *Macromolecules* **2004**, *37*, 4109; c) R. Caminiti, L. Pandolfi, P. Ballirano, *J. Macromol. Sci. B* **2000**, *39*, 481.
[22] a) J. Peet, E. Brocker, Y. H. Xu, G. C. Bazan, *Adv. Mater.* **2008**, *20*, **1882**; b) Y. Li, Y. Chen, X. Liu, Z. Wang, X. Yang, Y. Tu, X. Zhu, *Macromolecules* **2011**, *44*, 6370; c) A. R. Murphy, J. Liu, C. Luscombe, D. Kavulak, J. M. Fréchet, R. J. Kline, M. D. McGehee, *Chem. Mater.* **2005**, *17*, 4892; d) K. Faied, M. Frechette, M. Ranger, L. Mazerolle, I. Levesque, M. Leclerc, T.–A. Chen, R. D. Rieke, *Chem. Mater.* **1995**, *7*, 1390; e) S. D. D. V. Rughooputh, S. Hotta, A. J. Heeger, F. Wudl, *J. Polym. Sci., Part B: Polym. Phys.* **1987**, *25*, 1071.
[23] C. Joo, E. Özkumur, M. S. Ünlü, J. F. de Boer, *Biosens. Bioelectron.* **2009**, *25*, 275.
[24] a) G. von Maltzahn, A. Centrone, J.–H. Park, R. Ramanathan, M. J. Sailor, T. A. Hatton, S. N. Bhatia, *Adv. Mater.* **2009**, *21*, 3175; b) A. De La Zerda, C. Zavaleta, S. Keren, S. Vaithilingam, S. Bodapati, Z. Liu, J. Levi, B. R. Smith, T.–J. Ma, O. Orlkan, Z. Cheng, X. Chen, H. Dai, B. T. Khuri-Yakub, S. S. Gambhir, *Nat. Nanotechnol.* **2008**, *3*, 557; c) J. F. Lovell, C. S. Jin, E. Huynh, H. Jin, C. Kim, J. L. Rubinstein, W. C. W. Chan, W. Cao, L. V. Wang, G. Zheng, *Nat. Mater.* **2011**, *10*, 324.
[25] a) Y. Liu, K. Ai, J. Liu, M. Deng, Y. He, L. Lu, *Adv. Mater.* **2013**, *25*, 1353; b) K. Yang, H. Xu, L. Cheng, C. Sun, J. Wang, Z. Liu, *Adv. Mater.* **2012**, *24*, 5586; c) C. M. MacNeil, R. C. Coffin, D. L. Carroll, N. H. Levi-Polyachenko, *Macromol. Biosci.* **2013**, *13*, 28; d) Z. Zha, X. Yue, Q. Ren, Z. Dai, *Adv. Mater.* **2013**, *25*, 777; e) K. M. Au, Z. Lu, S. J. Matcher, S. P. Armes, *Adv. Mater.* **2011**, *23*, 5792; f) J. Zhou, Z. Lu, X. Zhu, X. Wang, Y. Liao, Z. Ma, F. Li, *Biomaterials* **2013**, *34*, 9584; g) J. Yang, J. Choi, D. Bang, E. Kim, E. –K. Lim, H. Park, J.–S. Suh, K. Lee, K.–H. Yoo, E.– K. Kim, Y.–M. Huh, S. Haam, *Angew. Chem. Int. Ed.* **2011**, *50*, 441; h) M. Chen, X. L. Fang, S. H. Tang, N. F. Zheng, *Chem. Comm.* **2012**, *48*, 8934; i) Z. B. Zha, Z. J. Deng, Y. Y. Li, C. H. Li, J. R. Wang, S. M. Wang, E. Z. Qu, Z. F. Dai, *Nanoscale* **2013**, *5*, 4462.